

# The effect of varying the duration of the butane/air pretreatment on the morphology and reactivity of $(\text{VO})_2\text{P}_2\text{O}_7$ catalysts

K.C. Waugh<sup>a,\*</sup>, Y.-H. Taufiq-Yap<sup>b</sup>

<sup>a</sup> Department of Chemistry, University of Manchester Institute of Science and Technology, Faraday Building,  
P.O. Box 88, Manchester M60 1QD, UK

<sup>b</sup> Department of Chemistry, Universiti Putra Malaysia, 43400 UPM Serdang, Selangor, Malaysia

## Abstract

Three vanadium pyrophosphate catalysts have been prepared by calcining vanadium hydrogen phosphate hemihydrate ( $\text{VOHPO}_4 \cdot 0.5\text{H}_2\text{O}$ ), prepared in an organic medium, for different lengths of time (40, 100 and 132 h) in a *n*-butane (0.75%)/air mixture at 673 K. The catalysts were designated VPO40, VPO100 and VPO132. Increasing the duration of reaction with *n*-butane/air mixture led to an increase in the total surface area from 21.3 (VPO40) to 24.9 m<sup>2</sup> g<sup>-1</sup> (VPO100) and 27 m<sup>2</sup> g<sup>-1</sup> (VPO132). It also led to the complete removal of the  $\text{VOPO}_4$  phase from catalysts VPO100 and VPO132, this  $\text{VOPO}_4$  phase having been seen as a minor component of catalyst VPO40. Scanning electron microscopy showed that longer periods of pretreatment in the *n*-butane/air mixture produced catalysts with increasing amounts of a characteristic rosette-type of agglomerate. Increasing the duration of the butane/air pretreatment at 673 K resulted in a lowering in the amount of oxygen desorbed on temperature programming, indicating that the butane/air pretreatment was effectively reducing. However, and apparently paradoxically, increasing the duration of the butane/air pretreatment resulted in an increase in the amount of oxygen removed from the catalysts by temperature programmed reduction in  $\text{H}_2$ , rising from 11 monolayers for VPO40 to 14 monolayers for VPO100 and to 15 monolayers for VPO132. All three catalysts showed a reduction peak with a maximum temperature of  $\sim 1000$  K for the removal of 11 monolayers of oxygen, while catalysts VPO100 and VPO132 showed a second reduction peak at  $\sim 1100$  K for the removal of an additional three (VPO100) and four monolayers (VPO132) of oxygen.

Published by Elsevier Science B.V.

**Keywords:** Monolayer; Temperature; Oxygen

## 1. Introduction

In the air oxidation of hydrocarbons such as benzene or butane to maleic anhydride over vanadium oxide based catalysts, three factors, either separately or in combination, could play an influential role in determining the overall selectivity of the reaction. These are: (i) the configuration of the adsorbate [1–4],

(ii) the surface morphology of the catalyst [1–4] and (iii) the nature of the oxidant [5–11].

There is a school of thought which holds that it is the (1 0 0) face of the  $(\text{VO})_2\text{P}_2\text{O}_7$  catalyst which is the selective face and that the geometric arrangement of the oxygen atoms on this face constrains the adsorbed butane molecule, held flat, into a configuration which pre-disposes it to form maleic anhydride by reaction with the surface oxygen anions [1–4].

In respect of the nature of the oxidant, Mars and van Krevelen were early proponents of the view that it was the oxygen of the crystal lattice which was

\* Corresponding author. Tel.: +44-161-200-4503;  
fax: +44-161-200-4430.  
E-mail address: ken.waugh@umist.ac.uk (K.C. Waugh).

involved in the selective and the unselective reactions [11]. They did not specify which lattice oxygen was selective and which was not; they simply ascribed selectivity to competitive rate processes. The role of the gas phase oxygen was considered to be that it should simply replace the lattice oxygen removed by reaction with the hydrocarbon. (Implicit in this model was the assumption that the transient oxygen species, which must exist on the surface of the oxide catalyst ( $\text{O}_2^-$ ,  $\text{O}^-$  and  $\text{O}^{2-}$ ) between chemisorption of the oxygen molecule at the anion vacancy and the ultimate healing of that vacancy, were extremely short lived and therefore were not involved in the reaction.)

That it is the oxygen of the  $(\text{VO})_2\text{P}_2\text{O}_7$  catalyst lattice which is the oxidant is beyond dispute. This has been demonstrated in an industrial process, the circulating riser reactor operated by Lerou et al. [12,13], in which the butane is oxidized anaerobically to maleic anhydride by the oxygen of the  $(\text{VO})_2\text{P}_2\text{O}_7$  lattice in one wing of the reactor, the oxygen depleted catalyst then being transported to another wing of the reactor where it is re-oxidized.

Since the oxygen can be removed from the lattice by reaction with the hydrocarbon, it might be considered that it should be available to the gas phase by thermal activation alone. Thermal desorption of oxygen from the lattice of the catalyst has not been observed for  $\text{Bi}_2(\text{MoO}_4)_3$  or  $\text{V}_2\text{O}_5$  catalysts [14] but has been observed for  $(\text{VO})_2\text{P}_2\text{O}_7$  catalysts [15]. The addition of P to the  $\text{V}_2\text{O}_5$  lattice therefore weakens the V–O bond strength and in doing so makes the catalyst more active and selective.

Taufiq-Yap and co-workers reported that approximately 1% by weight of the lattice oxygen, corresponding to 1.5 monolayers of oxygen anions, could be removed from the  $(\text{VO})_2\text{P}_2\text{O}_7$  lattice by thermal activation evolving in two peaks at 998 and 1023 K (Fig. 1) [16]. Fig. 2 is the anaerobic temperature programmed reaction profile obtained by passing *n*-butane in He (1.5% *n*-butane, 101 kPa,  $25 \text{ cm}^3 \text{ min}^{-1}$ ) over the catalyst while raising the temperature at  $5 \text{ K min}^{-1}$ . The figure shows that butene and butadiene are formed with identical kinetics and that the temperature dependence of their appearance is nearly the same as that of the thermal evolution

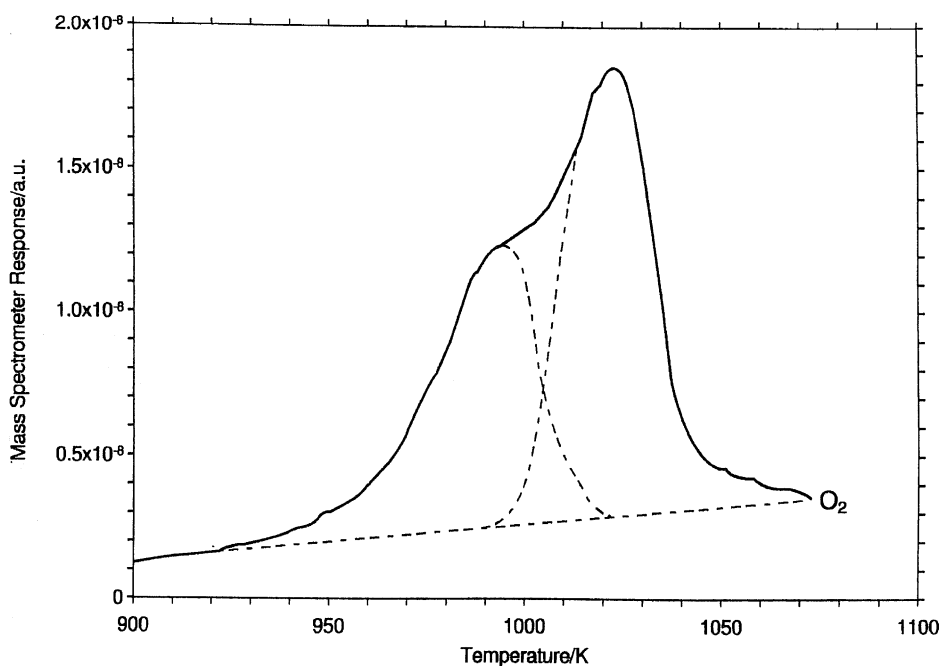


Fig. 1. Temperature programmed desorption  $\text{O}_2$  from a  $(\text{VO})_2\text{P}_2\text{O}_7$  catalyst pretreated in *n*-butane/air for 6 h.

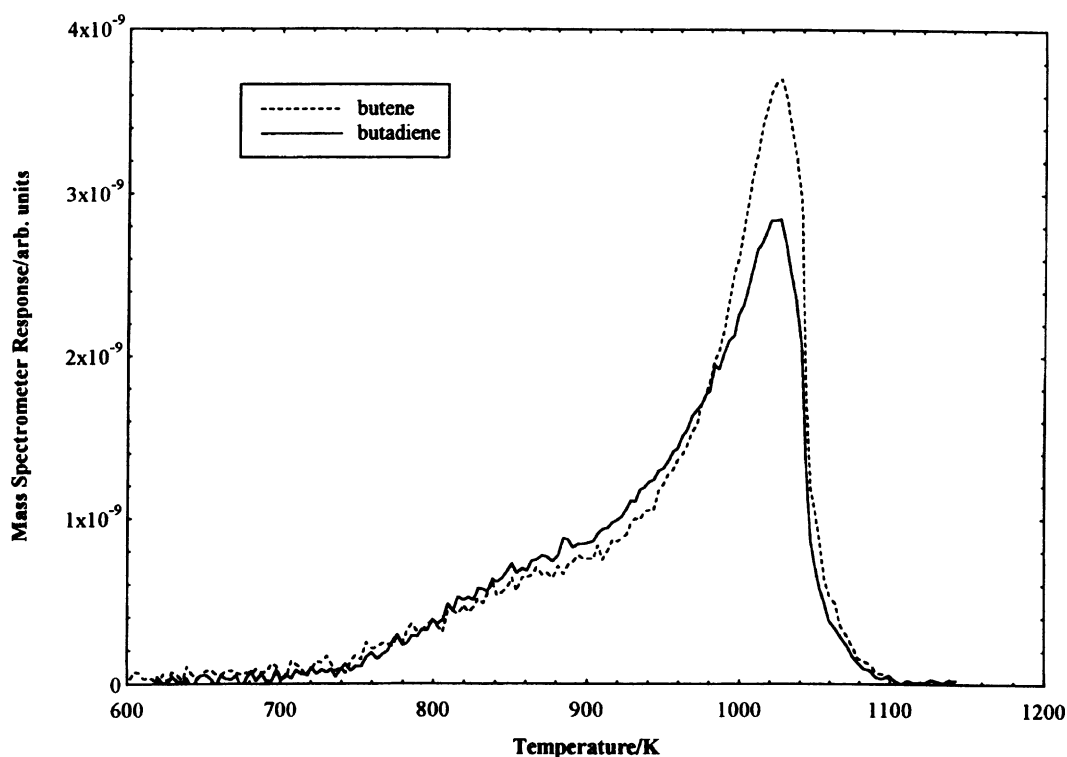


Fig. 2. *n*-Butane anaerobic temperature programmed reaction over the pre-oxidized  $(\text{VO})_2\text{P}_2\text{O}_7$  catalyst.

of  $\text{O}_2$  from the lattice. In addition the amount of oxygen required per gram of the catalyst for the production of butene and butadiene is exactly the same as that evolved by temperature programmed desorption at 998 and 1023 K. (See Table 1). We therefore

concluded that: (i) the rate determining step in the selective oxidation of butane to butene and butadiene was the migration of oxygen from the bulk of the vanadium pyrophosphate lattice to the surface and (ii) because of the correspondence between the

Table 1

Amounts of products formed in anaerobic temperature-programmed oxidation of *n*-butane, but-1-ene and 1,3-butadiene lattice on a  $(\text{VO})_2\text{P}_2\text{O}_7$  catalyst

Reactant	Products	$T_{\text{max}}$ (K)	Amount of products (mol g <sup>-1</sup> )	Lattice oxygen requirements for products (atom g <sup>-1</sup> )		Lattice oxygen desorbed (atom g <sup>-1</sup> )
<i>n</i> -Butane	Butene	1020	$1.2 \times 10^{20}$	$1.2 \times 10^{20}$	} $3.0 \times 10^{20}$	$2.2 \times 10^{20}$
	Butadiene	1020	$0.9 \times 10^{20}$	$1.8 \times 10^{20}$		
But-1-ene	Butadiene	990	$1.2 \times 10^{20}$	$1.2 \times 10^{20}$	} $3.0 \times 10^{20}$	$2.2 \times 10^{20}$
	Dihydrofuran	965	$0.6 \times 10^{20}$	$1.2 \times 10^{20}$		
	Furan	990	$0.2 \times 10^{20}$	$0.6 \times 10^{20}$		
But-1,3-diene	Dihydrofuran	970	$0.1 \times 10^{20}$	$0.1 \times 10^{20}$	} $0.7 \times 10^{20}$	$2.2 \times 10^{20}$
	Furan	1002	$0.3 \times 10^{20}$	$0.6 \times 10^{20}$		
	Maleic anhydride	1148	Unquantified	–		

amount of oxygen required for the oxidation of butane to butene and butadiene and the amount of oxygen desorbing from the lattice at 998 and 1023 K, the thermally stimulated evolving oxygen was 100% selective in the oxidation of butane to butene and butadiene [16,17]. Table 1 also shows that in the anaerobic temperature programmed oxidation of butene to butadiene and furan and of butadiene to furan and maleic anhydride there was a total correspondence between the oxygen which was thermally induced to desorb and the amount required for the given reactions. The temperature dependence of the production of butadiene and furan from butene and of furan and maleic anhydride on anaerobic oxidation closely resembled the temperature dependence of the evolution of oxygen from the vanadium pyrophosphate lattice [17].

These studies [16] also showed that if the butane was adsorbed flat on the surface, it was first dehydrogenated by the surface oxygen of the catalyst forming  $\text{H}_2\text{O}$ . The carbon skeleton which remained on the surface was then oxidized to  $\text{CO}_2$  by the oxygen of the lattice as it evolved at  $\sim 900\text{ K}$  [16]. The concept of the geometric arrangement of the surface oxygen anions of the  $(\text{VO})_2\text{P}_2\text{O}_7$  catalyst constraining the adsorbed butane molecule, lying flat on the surface, into a configuration which inevitably produces maleic anhydride, the crystallographic model of active centers [1–4], therefore does not apply.

A point that was lost in the earlier analysis of the data is that since the butene and the butadiene evolve simultaneously the butadiene is not formed by butene having been formed first and then desorbing, readSORbing and reacting. The butene and butadiene must be formed in nearly an identical mechanism by single end on adsorption of butane to the oxygen of the VPO lattice to form butadiene and by double end on adsorption to form butadiene. (It can easily be envisaged how that double end on adsorption of butane could lead to oxygen insertion and the formation of furan.)

The  $(\text{VO})_2\text{P}_2\text{O}_7$  catalyst used in these studies was prepared by refluxing  $\text{V}_2\text{O}_5$  with  $\text{H}_3\text{PO}_4$  in isobutyl alcohol at 393 K for 2 h, the dried filtrate being shown to be crystalline vanadium hydrophosphate hemihydrate ( $\text{VOHPO}_4 \cdot 0.5\text{H}_2\text{O}$ ) by X-ray diffraction [16]. The hemihydrate was then calcined in air at 673 K for 6 h followed by an additional 3 h at the same temperature in a *n*-butane/air mixture (0.75%

*n*-butane, 101 kPa,  $25\text{ cm}^3\text{ min}^{-1}$ ). It was considered that the time [16] that the duration of *n*-butane/air pretreatment was insufficient to produce the optimum  $(\text{VO})_2\text{P}_2\text{O}_7$  morphology, it being remembered that precursors calcined for less than 100 h yield what are regarded as “non-equilibrated” catalysts; a calcination time of more than 100 h is considered to produce “equilibrated” catalysts which are more stable under reaction conditions.

The purpose of the present study therefore is to investigate the effect of varying the duration of the *n*-butane/air pretreatment at 673 K upon the morphology and activity of the  $(\text{VO})_2\text{P}_2\text{O}_7$  catalyst produced.

## 2. Experimental

### 2.1. Catalysts preparation

The catalysts were prepared in organic medium by the following procedure. Vanadium pentoxide,  $\text{V}_2\text{O}_5$  (15.0 g from Fluka), was suspended by rapid stirring into a mixture of isobutyl alcohol ( $90\text{ cm}^3$ ) and benzyl alcohol ( $60\text{ cm}^3$ ). The vanadium oxide–alcohol mixture was refluxed for 3 h at 393 K, stirring throughout. The mixture was then cooled to room temperature overnight.  $\text{H}_3\text{PO}_4$  (85%) was added in such a quantity to obtain the desired P:V atomic ratio. The resulting solution was again heated to 393 K and maintained under reflux with constant stirring for 2 h. The slurry was then filtered, washed and dried overnight in an oven at 423 K.

The resulting precursor, which was shown to be a well crystallized  $\text{VOHPO}_4 \cdot 5\text{H}_2\text{O}$  by X-ray diffraction analysis, was then calcined under a flow of *n*-butane/air mixture (0.75% *n*-butane in air) at 673 K for 40, 100 and 132 h. The resulting catalysts were denoted by VPO40, VPO100 and VPO132, respectively.

### 2.2. Catalysts characterization

The total surface areas of the catalysts were measured by the Brunauer–Emmer–Teller (BET) method using nitrogen adsorption at 77 K. This was done using a Micromeritics ASAP 2000.

The X-ray diffraction (XRD) analyses were carried out using a Shimadzu diffractometer model XRD 6000 employing Cu  $\text{K}\alpha$  radiation to generate

diffraction patterns from powder crystalline samples at ambient temperature. SEM was done using a Jeol JSM-6400 electron microscope. The samples were coated with gold using a Sputter Coater. The photographs were captured using a Mamiya camera with Kodak Verichrome Pan 100 black and white negatives.

TPD and TPR analysis were done using a Micromeritics 2900 TPD/TPR apparatus utilizing a thermal conductivity detector (TCD).

### 3. Results and discussion

#### 3.1. Brunauer–Emmer–Teller surface area measurements

The surface areas of the catalysts are as follows:  $21.3 \text{ m}^2 \text{ g}^{-1}$  for VPO40,  $24.9 \text{ m}^2 \text{ g}^{-1}$  for VPO100 and  $27.0 \text{ m}^2 \text{ g}^{-1}$  for VPO132. Raising the calcination time increased the surface area. These values are also higher than those reported by Abon et al. [18–20].

The average particle size is therefore  $\sim 400 \text{ \AA}$  which will also be the mean pore diameter. The catalysts are therefore microporous.

#### 3.2. X-ray diffraction

Study of the XRD spectrum of the precursor showed the presence of  $\text{VOHPO}_4 \cdot 0.5\text{H}_2\text{O}$ , which was characterized by peaks at  $2\theta = 15.5, 19.6, 24.2, 27.1$  and  $30.4^\circ$ , as shown in Fig. 3 spectrum (a). These spectra are in good agreement with those reported for the  $\text{VOHPO}_4 \cdot 0.5\text{H}_2\text{O}$  phase [20–22]. The XRD spectra of the three catalysts which were prepared by calcination of the same precursor at 723 K under the flow of *n*-butane (0.75% *n*-butane in air) for different times on stream, i.e. 40, 100 and 132 h, are presented in Fig. 3 spectra (b), (c) and (d). These show that these catalysts have a well crystallized  $(\text{VO})_2\text{P}_2\text{O}_7$  phase. These materials are quite different from those obtained by Abon et al. [18–20], which are characteristic of a poorly crystallized  $(\text{VO})_2\text{P}_2\text{O}_7$  phase. However, our results are in agreement with those in which the amount of  $(\text{VO})_2\text{P}_2\text{O}_7$  phase increases with the activation time. A minor  $\text{VOPO}_4$  phase is detected on VPO40 while it was not on VPO100 and VPO132. The presence of  $(\text{VO})_2\text{P}_2\text{O}_7$  is characterized by the pyrophosphate lines at  $2\theta = 23, 28.45$  and  $29.94$ .

#### 3.3. Scanning electron microscopy

The results of scanning electron microscopy show the surface morphologies of the catalysts obtained after different calcination times. The principal structures of the catalysts are the same: they consist of plate-like crystals, which are arranged into the characteristic rosette-shape clusters. However, the amounts of these characteristic rosette-type agglomerates are different in all of the catalysts, as shown in Fig. 4(a–c).

The catalysts which had been calcined for the longest period of time, i.e. VPO132, appeared to have clearer and more prominent rosette-shape agglomerates when compared to its less calcined counterparts. There appeared to be a consistency whereby the amount of these rosette-type agglomerates increased with increasing calcination time. The rosette-type agglomerates are made up of agglomerates of  $(\text{VO})_2\text{P}_2\text{O}_7$  platelets that preferentially expose (100) crystal planes [23]. The increase in the surface area for catalysts which had undergone a longer calcination time could be explained by the increase in the number of platelets which formed the rosette structure.

#### 3.4. Oxygen desorption

The oxygen desorption spectra shown in Fig. 5 were obtained by pretreating the  $(\text{VO})_2\text{P}_2\text{O}_7$  catalysts by heating them to 673 K in an oxygen flow ( $101 \text{ kPa}, 25 \text{ cm}^3 \text{ min}^{-1}$ ) and holding them under that flow at 673 K for 1 h before cooling them to ambient temperature. The flow was then switched to helium ( $1 \text{ bar}, 25 \text{ cm}^3 \text{ min}^{-1}$ ) and the temperature was raised ( $10 \text{ K min}^{-1}$ ) to 1100 K following the conductivity of the eluted gas. Peaks obtained derived from the evolution of oxygen from the catalysts, it having been shown previously [16] that the pretreatment in oxygen at 673 K removed all the adsorbed  $\text{H}_2\text{O}$ . Peaks are observed at 978 K with a shoulder at 938 K for VPO40.

The total amount of oxygen desorbed is  $2.0 \times 10^{20} \text{ atom g}^{-1}$  (Table 2), and this is almost the same as we reported previously for a calcination of 6 h in a mixture of *n*-butane/air [17]. However, the desorption temperatures have been slightly reduced from 1023 and 998 K. This amount on a catalyst with surface area of  $21.3 \text{ m}^2 \text{ g}^{-1}$ , corresponds to a coverage of  $9.4 \times 10^{14} \text{ atom cm}^{-2}$  on the surface of the

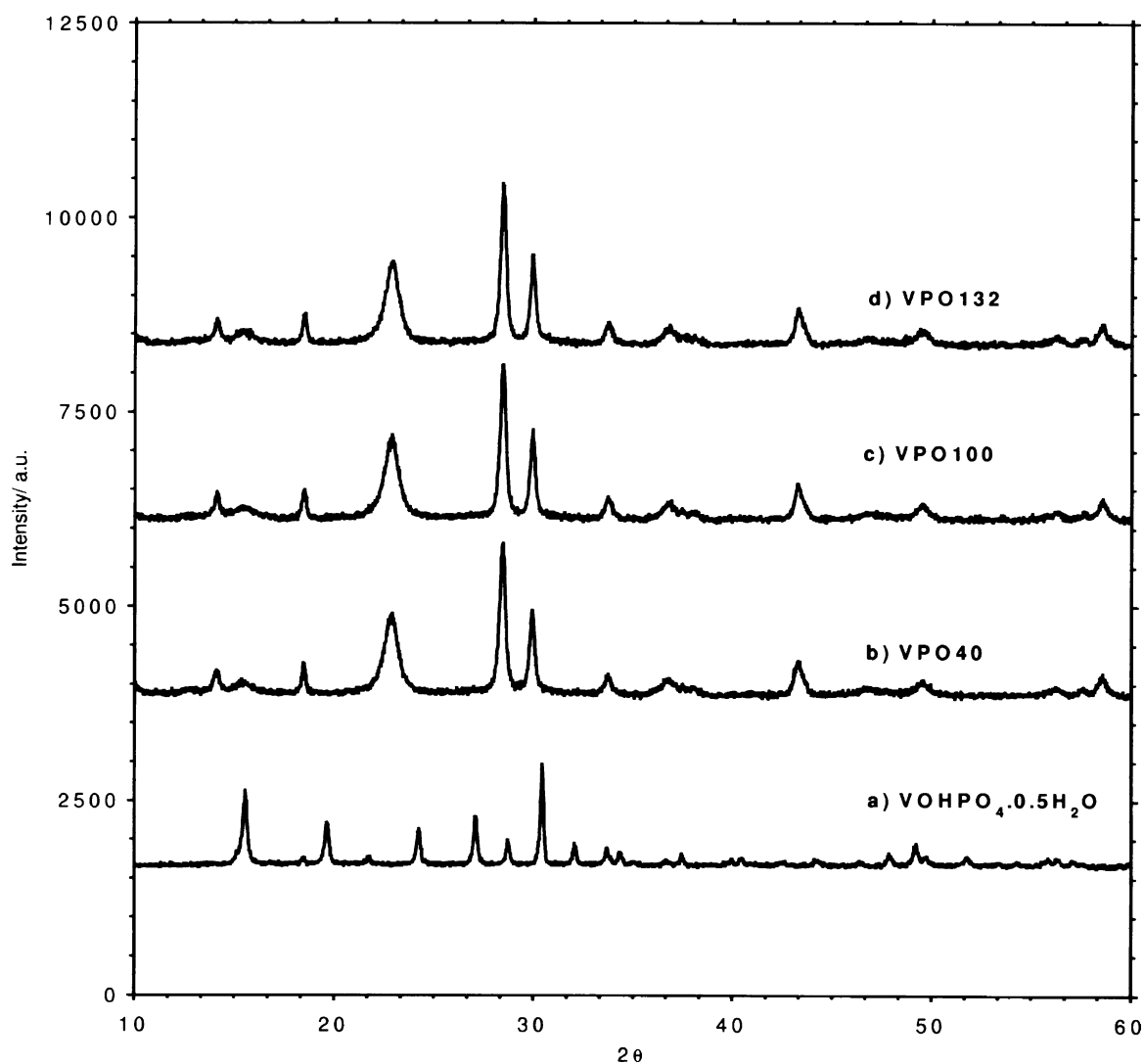


Fig. 3. X-ray diffraction spectra of  $\text{VOHPO}_4 \cdot 0.5\text{H}_2\text{O}$ , VPO40, VPO100 and VPO132.

Table 2

Total number of oxygen atoms desorbed from the catalysts by  $\text{O}_2$  TPD

Catalyst <sup>a</sup>	$T_{\text{max}}$ (K)	Oxygen atoms desorbed from the catalyst ( $\text{mol g}^{-1}$ )	Total oxygen atoms desorbed ( $\text{atom g}^{-1}$ )	Coverage ( $\text{atom cm}^{-2}$ )	Monolayers of oxygen removed <sup>b</sup>
VPO40	978	$1.7 \times 10^{-4}$	$2.0 \times 10^{20}$	$9.4 \times 10^{14}$	1.3
	938				
VPO100	937	$8.3 \times 10^{-5}$	$9.9 \times 10^{19}$	$3.9 \times 10^{14}$	0.6
VPO132	937	$8.4 \times 10^{-5}$	$1.0 \times 10^{20}$	$3.7 \times 10^{14}$	0.5

<sup>a</sup> Surface area: VPO40  $21.3 \text{ m}^2 \text{ g}^{-1}$ , VPO100  $24.9 \text{ m}^2 \text{ g}^{-1}$ , VPO132  $27.0 \text{ m}^2 \text{ g}^{-1}$ .

<sup>b</sup> The monolayers of oxygen removed are calculated by dividing the oxygen coverage by  $7 \times 10^{14} \text{ atom cm}^{-2}$ —the stoichiometric value of monolayer oxygen coverage.



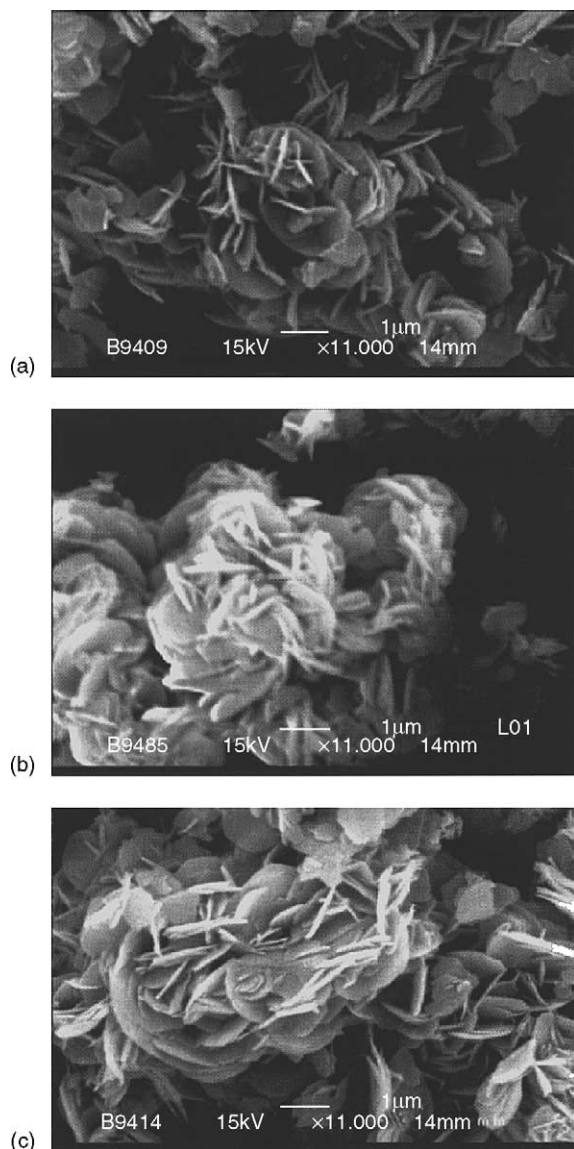


Fig. 4. SEM micrographs of (a) VPO40, (b) VPO100 and (c) VPO132.

(VO)<sub>2</sub>P<sub>2</sub>O<sub>7</sub> catalyst. This coverage corresponds to more than a monolayer of lattice oxygen.

For catalysts calcined for longer times (catalysts VPO100 and VPO132) two salient observations can be made. Firstly, the amount of oxygen desorbed is half that desorbed from catalyst VPO40, being  $9.9 \times 10^{19}$  for VPO100 and  $1.0 \times 10^{20}$  atom g<sup>-1</sup> for VPO132. This corresponds to coverages of  $3.9 \times 10^{14}$  and

$3.7 \times 10^{14}$  atom cm<sup>-2</sup> or the removal of the equivalent of half a monolayer of the surface oxygen of the lattice. The most likely route for this loss of oxygen from these catalysts is the formation of crystallographic shear planes [24]. This observation of the longer times of calcinations in the *n*-butane/air mixture producing catalysts which desorb less oxygen is consistent with one of the conclusions of a previous report, namely that the role of the *n*-butane/air pretreatment is to remove the unselective oxygen [16]; temperature programmed reaction studies have shown that the shorter calcination time of 6 h leaves at least two monolayer equivalents of unselective oxygen [16]. Our conclusion that the *n*-butane/air pretreatment actually reduces the (VO)<sub>2</sub>P<sub>2</sub>O<sub>7</sub> catalyst accords with those of [25,26] who state that the plates formed by the *n*-butane/air pretreatment are actually reduced phases of VPO.

The second important point to note is that increasing the calcination time to 100 and 132 h results in the loss of high temperature desorption state having a  $T_m$  of 978 K (and the concomitant loss in the total amount of oxygen desorbed); the low-temperature state ( $T_m = 938$  K) remains in roughly the same amount.

The oxygen desorption peaks from catalysts VPO100 and VPO132 are symmetric and are therefore second-order [27]. The rate of desorption is therefore given by

$$-d[O(s)]/dt = Ae^{-E/RT}[O(s)]^2, \quad (1)$$

where  $[O(s)]$  is the surface oxygen atom concentration (mol cm<sup>-2</sup>),  $t$  the time (s),  $A$  the Arrhenius pre-exponential term (cm<sup>2</sup> mol<sup>-1</sup> s<sup>-1</sup>),  $E$  the desorption activation energy (J mol<sup>-1</sup>),  $R$  the gas constant (J K<sup>-1</sup> mol<sup>-1</sup>) and  $T$  the temperature (K). Since the rate of desorption,  $-d[O(s)]/dt$ , is equal to the height of the peak,  $h$  (cm) at any temperature,  $T$  (K) multiplied by some calibration constant  $K'$ , and since the surface oxygen atom concentration  $[O(s)]$  at that temperature is given by the area (cm<sup>2</sup>) of the peak at that temperature multiplied by some other calibration constant  $K''$ , then Eq. (1) becomes

$$K'h = Ae^{-E/RT}(K'' \text{ area})^2 \quad (2)$$

or

$$\frac{h}{\text{area}^2} = Ae^{-E/RT} \frac{K}{(K'')^2}. \quad (3)$$

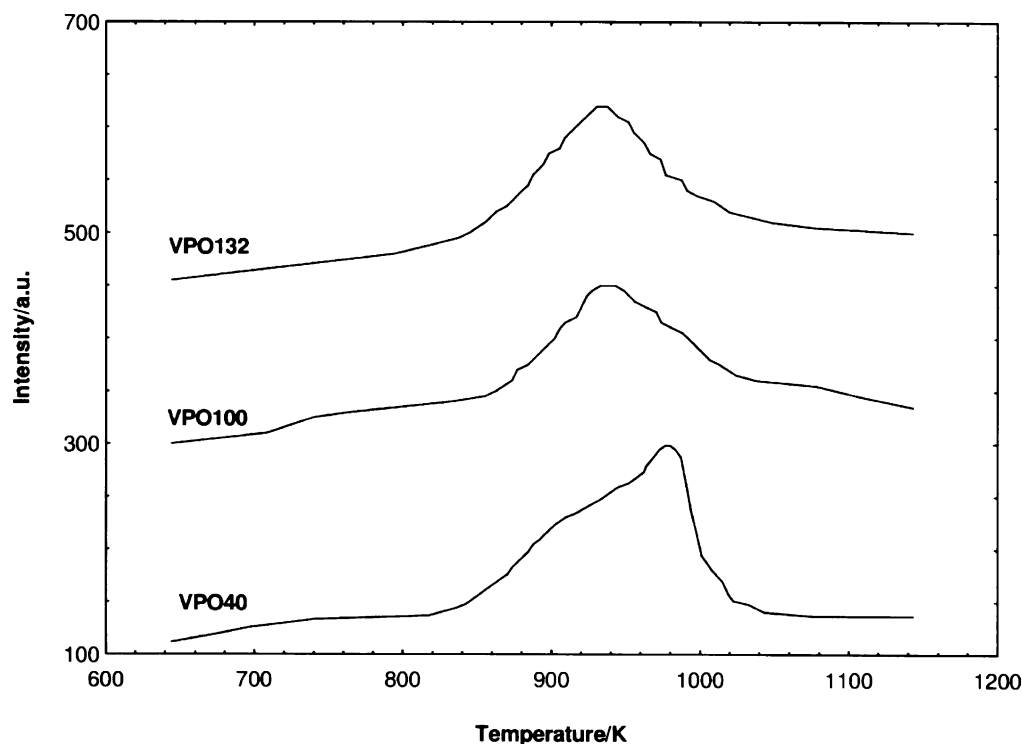


Fig. 5. Temperature programmed desorption of O<sub>2</sub> from VPO40, VPO1000 and VPO132.

A plot of  $\ln(h/\text{area}^2)$  versus  $1/T$  constitutes line shape analysis of the peak and provides the desorption activation energy without the need for calibration or assumptions about the value of the desorption pre-exponential factor. The value so obtained is  $97 \text{ kJ mol}^{-1}$ .

### 3.5. Temperature-programmed reduction in H<sub>2</sub>/Ar

Additional information as to the nature and the oxidizing species available from the VPO catalysts was obtained by TPR in H<sub>2</sub>/Ar stream (10% H<sub>2</sub>) using a fresh sample of catalyst and raising the temperature from room temperature to 1173 K at  $20 \text{ K min}^{-1}$  in that stream. The TPR profiles in H<sub>2</sub> so obtained are shown in Fig. 6. Table 3 lists the peak maximum temperatures, the amounts of oxygen removed in each peak and the derived reduction activation energies.

There are several points to note from these temperature programmed reduction profiles. These are:

(i) regardless of the duration of pretreatment in the *n*-butane/air mixture, the amount of oxygen removed by H<sub>2</sub> at the peak maximum of  $\sim 1010 \text{ K}$  is roughly the same; (ii) the amount of oxygen removed by H<sub>2</sub> in this peak is  $\sim 2 \times 10^{20} \text{ atom g}^{-1}$  (equivalent to 11 monolayers) which is a factor of 10 greater than that removed by thermal desorption for catalyst VPO40 and 20 greater than that removed by TPD from catalysts VPO100 and VPO132; (iii) while reaction with H<sub>2</sub> induces the removal of a greater amount of oxygen from the lattice than can be removed thermally, the peak maximum temperature of the reduction is higher than that of the thermally induced desorption, suggesting that the rate-determining step in both is the diffusion of oxygen through the lattice (the line shapes of the 1010 K H<sub>2</sub>-TPR peaks shown in Fig. 6 are characteristic of zero-order reaction [28]), exhibiting an exponentially increasing edge and a near-vertical decrease after the maximum. This conclusion of the reaction being zero-order is consistent with the large amount of oxygen removed from the lattice (11 monolayers



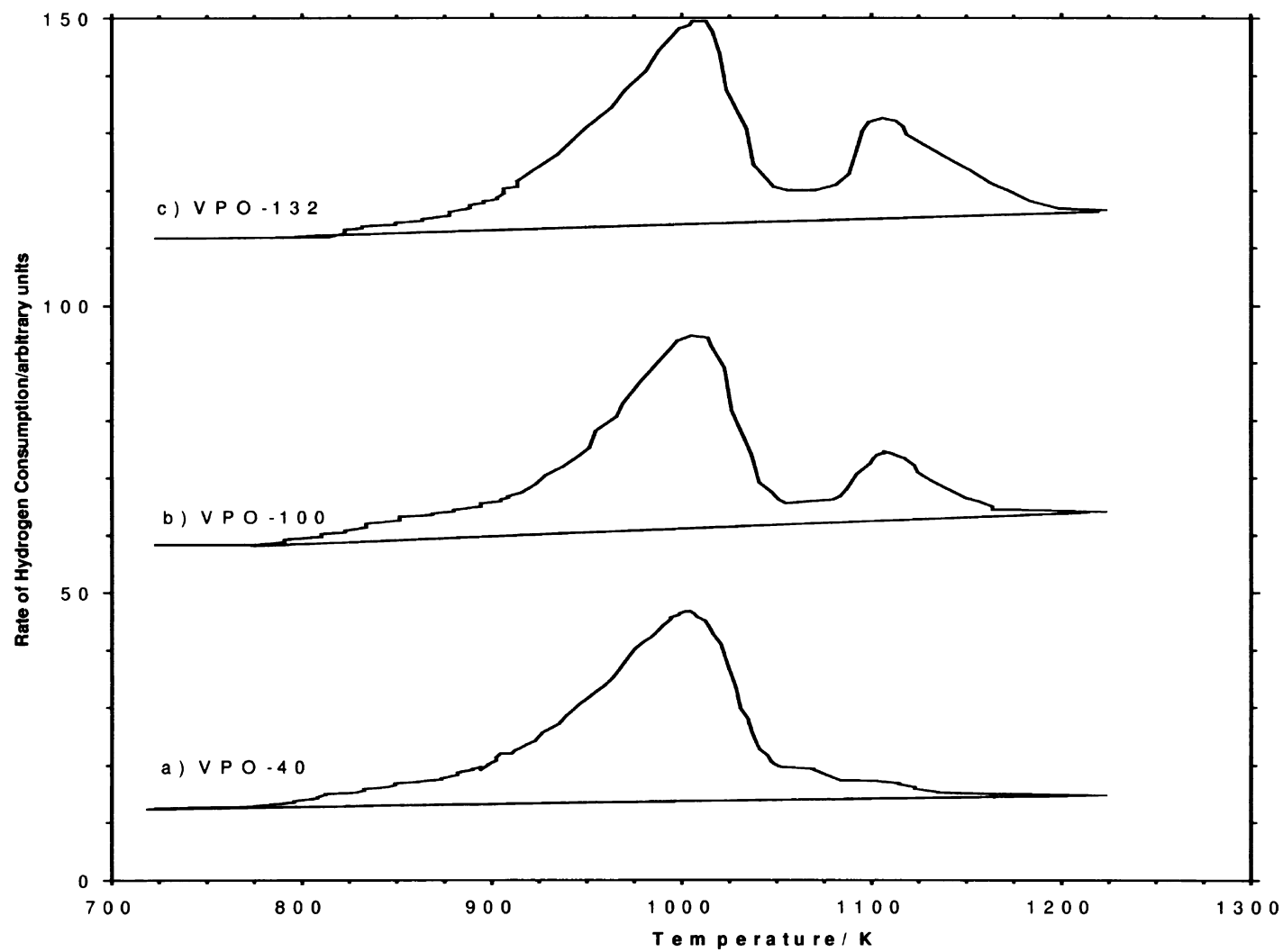


Fig. 6. Temperature programmed reaction of  $H_2$  with VPO40, VPO100 and VPO132.

Table 3

Total number of oxygen atoms removed from VPO40, VPO100 and VPO132 catalysts by reduction in H<sub>2</sub>/Ar

Peaks <sup>a</sup>	<i>T</i> <sub>max</sub> (K)	Reduction activation energy <i>E</i> <sub>r</sub> (kJ mol <sup>−1</sup> )	Oxygen atoms removed from the catalyst		Coverage (atom cm <sup>−2</sup> )	Monolayers of oxygen removed <sup>b</sup>
			mol g <sup>−1</sup>	atom g <sup>−1</sup>		
VPO40						
1	1003	174	$2.7 \times 10^{-3}$	$1.6 \times 10^{21}$	$7.7 \times 10^{15}$	11.0
VPO100						
1	1009	175	$3.3 \times 10^{-3}$	$2.0 \times 10^{21}$	$8.0 \times 10^{15}$	11.0
2	1109	192	$7.3 \times 10^{-4}$	$4.4 \times 10^{20}$	$1.8 \times 10^{15}$	2.6
Total oxygen atoms removed			$4.0 \times 10^{-3}$	$2.4 \times 10^{21}$	$9.8 \times 10^{15}$	13.6
VPO132						
1	1009	175	$3.7 \times 10^{-3}$	$2.2 \times 10^{21}$	$8.1 \times 10^{15}$	11.0
2	1109	192	$1.2 \times 10^{-3}$	$7.4 \times 10^{20}$	$2.7 \times 10^{15}$	3.9
Total oxygen atoms removed			$4.9 \times 10^{-3}$	$2.9 \times 10^{21}$	$1.1 \times 10^{16}$	14.9

<sup>a</sup> Surface area: VPO40 21.3 m<sup>2</sup> g<sup>−1</sup>, VPO100 24.9 m<sup>2</sup> g<sup>−1</sup>, VPO132 27.0 m<sup>2</sup> g<sup>−1</sup>. Weight of catalyst = 0.03 g.<sup>b</sup> The monolayers of oxygen removed are calculated by dividing the oxygen coverage by  $7 \times 10^{14}$  atom cm<sup>−2</sup>—the stoichiometric value of monolayer oxygen coverage.

equivalent). A plot, therefore, of the logarithm of the rate of reaction (peak height) versus  $1/T$  constitutes line shape analysis of this peak; it provides an activation energy of 119 kJ mol<sup>−1</sup> for reduction of the catalyst by H<sub>2</sub>. This value is the same for all three catalysts so that varying the time of pretreatment in the *n*-butane/air mixture has no effect on the kinetics of the reduction of this phase; (iv) increasing the duration of the *n*-butane/air pretreatment from 40 to 100 h and 132 h results in the development of a new peak at 1100 K in the H<sub>2</sub>-TPR profile; (v) the amount of oxygen removed in this high-temperature state increases with an increase in the duration of the *n*-butane/air pretreatment, having a value of  $4.4 \times 10^{20}$  atom g<sup>−1</sup> (2.6 monolayer equivalent) for 100 h pretreatment, rising to  $7.4 \times 10^{20}$  atom g<sup>−1</sup> (3.9 monolayer equivalent) for 132 h pretreatment.

The result that the longer the period of *n*-butane/air pretreatment the more oxygen is removed from the lattice by reaction with H<sub>2</sub> appears to conflict with the observation that less oxygen is available from the lattice thermally on increasing the time of *n*-butane/air pretreatment. However, it is clear from the fact that reduction in H<sub>2</sub> removes >10 times the amount of lattice oxygen which can be removed thermally, that the transition states of the two processes are quite different.

The SEM pictures shown in Fig. 4 show that treatment in the *n*-butane/air mixtures for longer periods of time produces catalysts with higher total areas by developing more of the clearly defined rosette-type structure. Indeed since the same amount of oxygen is removed in the 1010 K peak by TPR in H<sub>2</sub>, and since this is the dominant amount of oxygen removed, it can be concluded that the surface/bulk morphologies of catalysts VPO40, VPO100 and VPO132 are largely the same. However it can be seen in the development of a new H<sub>2</sub>-TPR peak at 1100 K for catalysts VPO100 and VPO132 that the extended duration of *n*-butane/air pretreatment produces a new phase, which, though the H<sub>2</sub>-TPR peak maximum is higher than for VPO40 (indicating a stronger VO bond strength) nevertheless still allows more oxygen to be removed from the lattice.

This new phase and the additional amount of oxygen it provides from the lattice might well be the source of the higher selectivity produced by longer periods of *n*-butane/air pretreatment.

#### 4. Conclusions

- (1) Increasing the length of time of pretreatment of vanadyl pyrophosphate catalysts to a *n*-butane/air mixture (0.75% *n*-butane) at 673 K increases the

surface area of the catalyst and changes the surface and bulk morphologies into one in which more oxygen can be removed from the lattice by reaction with  $H_2$ .

- (2) The significant difference between the catalysts produced for the longest time of pretreatment (132 h) and the shortest (40 h) is that the longest time of pretreatment produces a new phase which reacts with  $H_2$  at an onset temperature of 1100 K in addition to the majority phase which is present in all catalysts whatever time of exposure to the *n*-butane/air mixture. This phase reacts with  $H_2$  at an onset temperature of 800 K and with identical kinetics for all three catalysts.
- (3) Apparently paradoxically, the least amount of oxygen can be removed from the catalysts thermally after the longest period *n*-butane/air pretreatment. This difference is rationalized in the markedly different transition state required for thermal evolution of  $O_2$  compared with that for  $H_2$  reduction of the surface, a fact borne out by the observation that  $H_2$  reduction removes >10 times the oxygen from the lattice than is available thermally.
- (4)  $H_2$  temperature programmed reduction is a reliable method of evaluation of catalysts for alkane activation since the initial step in the activation of alkanes is C–H scission, the transition state for which will be similar to that for H–H bond scission.
- (5) Since we have shown that the lattice oxygen is 100% selective in the oxidation of butane to butanes and of butanes to furan and maleic anhydride, it is predicted that the longer duration of butane/air pretreatment will produce a more active and more selective catalyst.

## Acknowledgements

Financial assistance from Malaysian Ministry of Science, Technology and Environment is gratefully acknowledged.

## References

- [1] J. Ziolkowski, E. Bordes, P. Courtine, *J. Catal.* 26 (1984) 249.
- [2] J. Ziolkowski, E. Bordes, P. Courtine, *Stud. Sci. Surf. Catal.* 55 (1991) 625.
- [3] J. Ziolkowski, E. Bordes, P. Courtine, *J. Mol. Catal.* 84 (1993) 307.
- [4] E. Bordes, *Catal. Today* 16 (1993) 27.
- [5] J. Lucas, H.D. Vandervell, K.C. Waugh, *J. Chem. Soc., Faraday Trans. 1* (77) (1981) 15.
- [6] J. Lucas, H.D. Vandervell, K.C. Waugh, *J. Chem. Soc., Faraday Trans. 1* (77) (1981) 31.
- [7] R.W. Petts, K.C. Waugh, *J. Chem. Soc., Faraday Trans. 1* (78) (1982) 803.
- [8] A. Bielanski, J. Haber, *Oxygen in Catalysis*, Dekker, New York, 1991, p. 395.
- [9] M. Witko, E. Broclawik, J. Haber, *J. Mol. Catal.* 26 (1984) 249.
- [10] P.A. Agaskar, L. De Caul, R.K. Grasselli, *Catal. Lett.* 23 (1994) 339.
- [11] J. Mars, D.W. van Krevelen, *Chem. Eng. Sci. Spec. Suppl.* 3 (1954) 41.
- [12] J.J. Lerou, P. Mills, Precision process technology, in: M.P.C. Weijnen, A.A. Drinkenburg (Eds.), Kluwer Academic, Dordrecht/Norwell, MA, 1993, p. 175.
- [13] J.J. Lerou, K.M. Ng, *Chem. Eng. Sci.* 51 (1996) 1595.
- [14] Y.H. Taufiq-Yap, Ph.D. Thesis, UMIST, Manchester, UK, 1997.
- [15] I. Ramli, Ph.D. Thesis, UMIST, Manchester, UK, 2000.
- [16] B.H. Sakakini, Y.H. Taufiq-Yap, K.C. Waugh, *J. Catal.* 189 (2000) 253.
- [17] B.H. Sakakini, Y.H. Taufiq-Yap, K.C. Waugh, *Catal. Lett.* 48 (1997) 105.
- [18] M. Abon, K.E. Bere, A. Tuel, P. Delichere, *J. Catal.* 156 (1995) 28.
- [19] M. Abon, J.C. Volta, *Appl. Catal.* 157 (1997) 173.
- [20] J.M. Hermann, P. Vernoux, K. Bere, M. Abon, *J. Catal.* 167 (1997) 106.
- [21] N.H. Batis, H. Batis, A. Ghorbel, J.C. Vedrine, J.C. Volta, *J. Catal.* 128 (1991) 248.
- [22] S. Albonetti, F. Cavani, F. Trifiro, P. Venturoli, G. Calestani, M.L. Granados, J.L.G. Fierro, *J. Catal.* 160 (1996) 52.
- [23] C.J. Kiely, S. Sajip, I.J. Ellison, M.T. Sananes, G.J. Hutchings, *J.C. Volta, Catal. Lett.* 33 (1995) 357.
- [24] P.L. Gai, K. Kourtakakis, *Science* 67 (1995) 661.
- [25] P.L. Gai, *Acta Cryst. B* 53 (1997) 346.
- [26] P.L. Gai, K. Kourtakakis, D.R. Coulson, G.C. Sonnichsen, *J. Phys. Chem.* 101 (1997) 9916.
- [27] P.A. Redhead, *Vacuum* 12 (1962) 203.
- [28] R.J. Madix, *Catal. Rev. Sci. Eng.* 15 (1997) 293.